Precipitation Patterns in a Cyclone

By
Donald L. Hadley

Department of Atmospheric Science
Colorado State University
Fort Collins, Colorado

Colorado State University

Department of Atmospheric Science

Paper No. 157

PRECIPITATION PATTERNS IN A CYCLONE

by

D. L. Hadley

This report was prepared with support
from Contract OWRR 14-01-0001-1887

from the

Office of Water Resources Research
and the State of Colorado
Project Leader: J. L. Rasmussen

Department of Atmospheric Science
Colorado State University
Fort Collins, Colorado

March, 1970

Atmospheric Science Paper No. 157

ABSTRACT

The major storm through the Midwest during the period 26 January to 28 January, 1967 was investigated to determine the cause of the narrow belt of exceedingly heavy snowfall, and to illustrate the relationship between the broad scale air motion and the synoptic and mesoscale precipitation pattern. The three-dimensional wind field has been studied by means of isentropic analyses; and the precipitation patterns by means of mesoanalyses of the Weather Bureau's hourly precipitation data.

It was found that a low level wind maximum and the conservation of potential vorticity of a parcel of air involved in the upglide motion over the warm front were a key to the production of convective instability and the resulting mesoscale precipitation pattern.

The atmospheric water balance was calculated for a small section of this storm with good results.

ACKNOWLEDGEMENTS

The author wishes to express his gratitude to Professor James L. Rasmussen for his invaluable counsel and helpful suggestions during the execution of this research and preparation of this manuscript.

This work was partially funded by the State of Colorado and the Office of Water Resources Research, contract number OWRR 14-01-0001-1887.

Sincere thanks also go to Mrs. Sue Kerbs who typed the manuscript.

TABLE OF CONTENTS

LIST OF TABLES

LIST OF FIGURES

List of Figures Continued

CHAPTER I

INTRODUCTION

The generalized patterns of precipitation in midlatitude depressions are widely accepted. These patterns, based on the Norwegian School model call for a large shield of light but more or less continuous precipitation ahead of the advancing warm front, and a narrow band of heavy, but of short duration, precipitation along the cold front. These precipitation patterns are a result of dynamically induced broadscale ascent. However, often there are observed significant features in the precipitation distribution on the sub-synoptic scale which renders a much more complicated pattern than that ascribed by the model.

Wexler and Atlas (1959) found through detailed radar analysis of wintertime cyclones that on the northerly side of an easterly moving depression there was an abrupt change from a relatively uniform echo pattern to a cellular pattern. This abrupt change, they reasoned was caused by the advection of dry air ahead of the upper level trough to the right of the jet. This dry subsiding air in combination with lower saturated air forms a convectively unstable layer which is involved in the upglide motion over the warm front.

Browning and Harrold (1969) found that the dynamically induced ascent was responsible for triggering a pre-existing region of high level potential instability thereby producing the small-scale convective generator cells detected with an AN/TPS-10 radar. These high level cells caused the banded structure in the precipitation pattern of the travelling wave depression.

Sawyer (1952) concluded that the sub-synoptic scale patterns of precipitation were produced either by small scale overturning associated with vertical instability or forced orographic lifting.

During the period 26-28 January, 1967, a major wintertime cyclone moved northeastward across the central United States. Embedded within the vast precipitation shield accompanying this depression was a small area of greater intensity precipitation. This localized area can be traced through at least 3 consecutive map times, a duration of more than 30 hours. The integrated effect of this subsynoptic scale phenomenon was a long, narrow belt, approximately 550 miles long and 120 miles wide, of unprecedented snowfall through the upper midwest. (Smith, 1967: Bunting and Lamb, 1968) (fig. 1). Record snows were commom from western Illinois to lower Michigan.

The aims of this investigation are twofold. First to describe the broad scale flow pattern around this depression, and second, and most important, to describe on the subsynoptic scale the particular mechanism for producing the necessary vertical instability resulting in the precipitation anomaly.

This particular storm was selected for study for numerous reasons. First, the Midwest has a great density of upper air soundings, surface stations and hourly precipitation gauges. Second, the terrain is relatively flat and orographically induced precipitation can be considered as negligible, leaving only localized areas of vertical instability as a generating mechanism of the precipitation anomaly. Third, and finally, this storm dramatically illustrates the tremendous economic and physical hardships resulting from such a storm and points out the need for more accurate forecasting of mesoscale phenomenon.

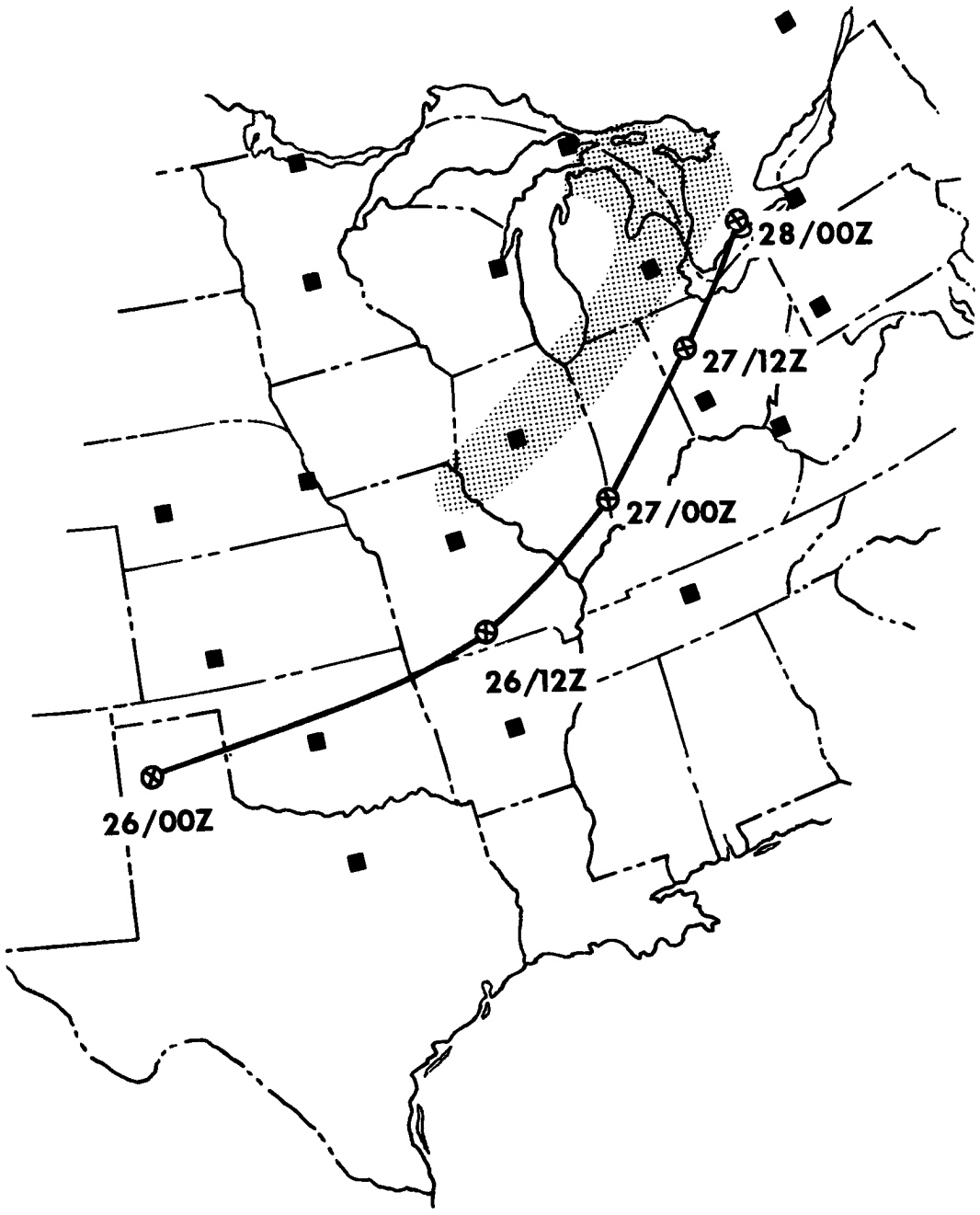

Figure 1. Track of the low pressure center. Small squares denote radiosonde station locations used in the analysis. Gray shaded area is region of heavy precipitation.

CHAPTER II

SYNOPTIC DEVELOPMENT

At the 500 mb level at 26/00Z a rapidly moving short wave crossed the Rockies and intensified in the lee of the mountains (refer to fig. 2 for surface, 850 mb, 500 mb charts). During the next 24 hours the trough continued to develop so that by 27/00Z it had formed a closed low. The closed low then slowly moved eastward across the eastern half of the United States.

At the 850 mb level between 26/00Z and 26/12Z, the combined effect of the deepening of the depression over the central United States and the building of a ridge over the upper Great Plains are resulted in a core of high speed winds north and west of storm center. The low level wind maximum attained its greatest velocity of over 50 knots at the 27/00Z observation period.

On the surface, the positioning of the 500 mb shortwave over the low level baroclinic zone associated with an already existing cold front resulted in an unstable wave forming on that cold front. The wave rapidly developed so that by 27/12Z it had reached its greatest intensity. By 28/00Z the occlusion process had begun as the storm center moved across the Great Lakes into Canada.

In the early stages of the cyclone development, the main precipitation area was located north of the warm front, extending northeastward from the low center in the Oklahoma-Arkansas area. As the cyclone matured the main area of precipitation was located to the north and west of the storm center.

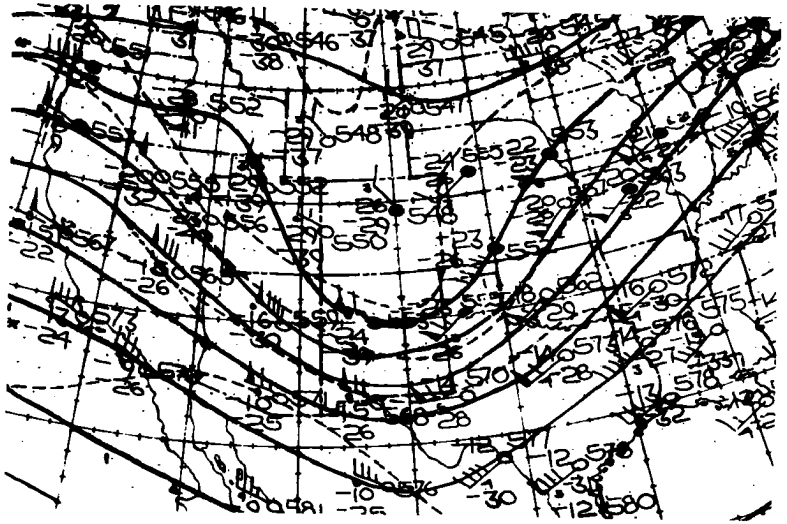

500mb

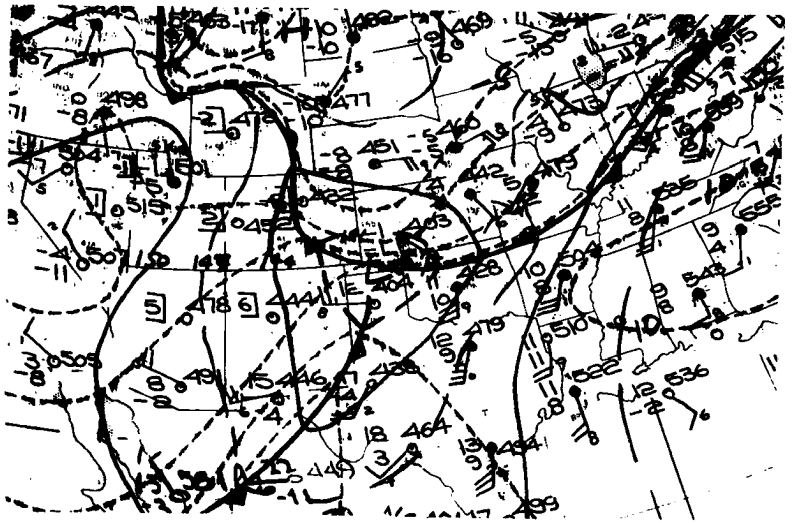

850mb

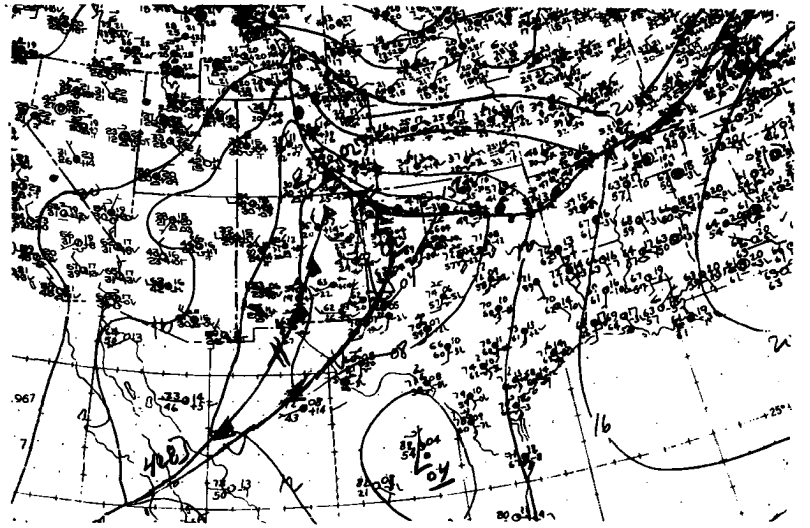

SURFACE

Figure 2a. Surface, 850 mb, and 500 mb for 26 Jan 1967 00Z showing development of the storm system.

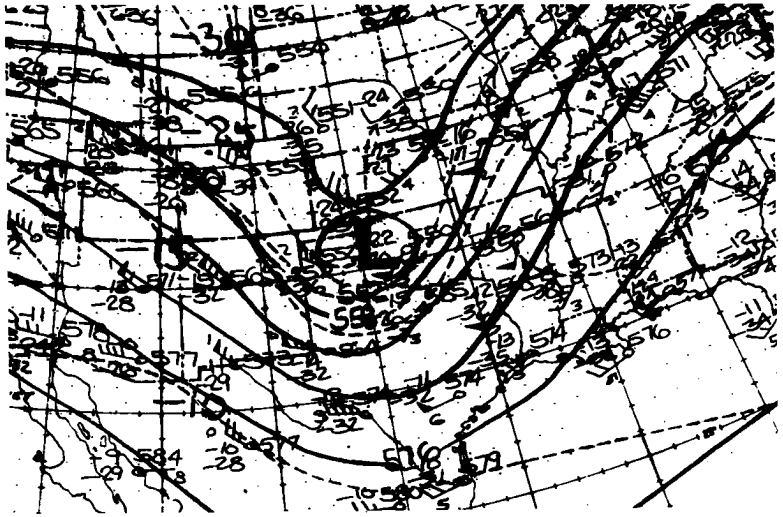

500mb

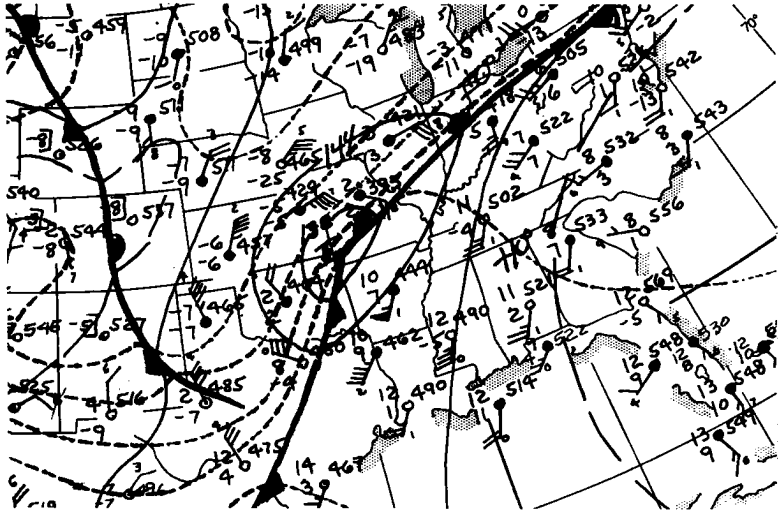

850mb

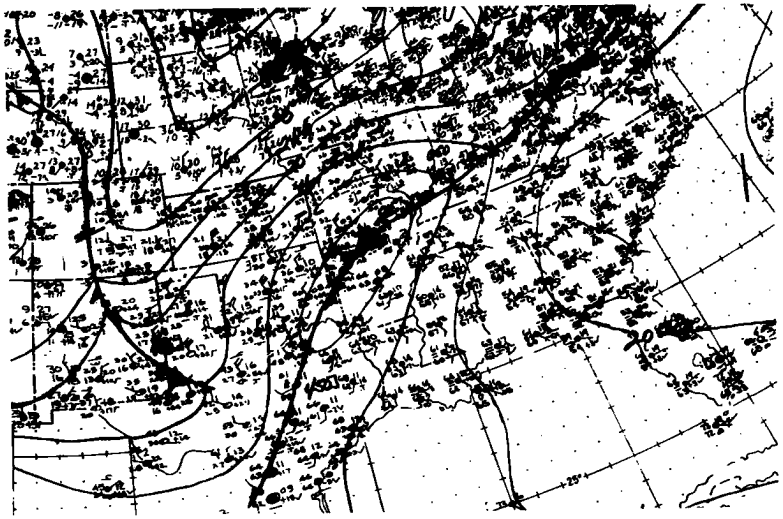

SURFACE

Figure 2b Surface, 850 mb, and 500 mb for 26 Jan 1967 12Z showing development of the storm system.

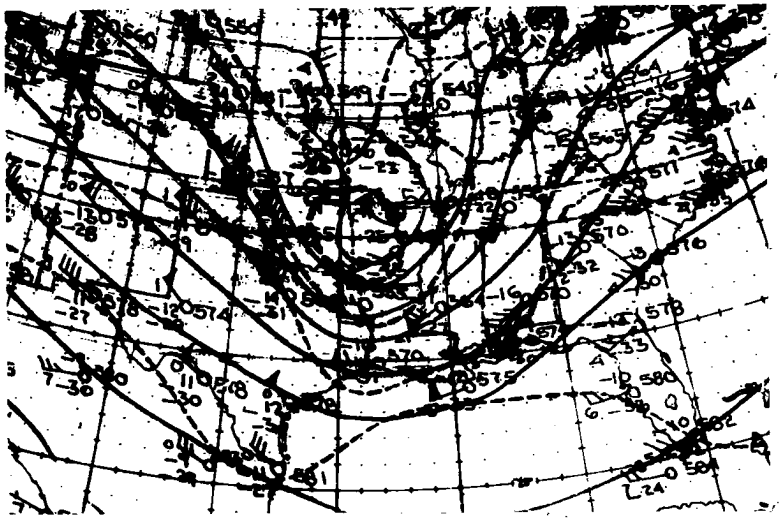

500mb

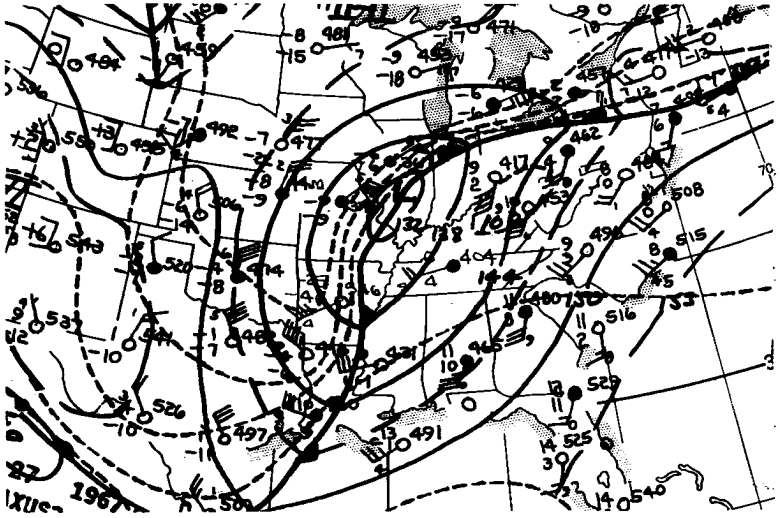

850mb

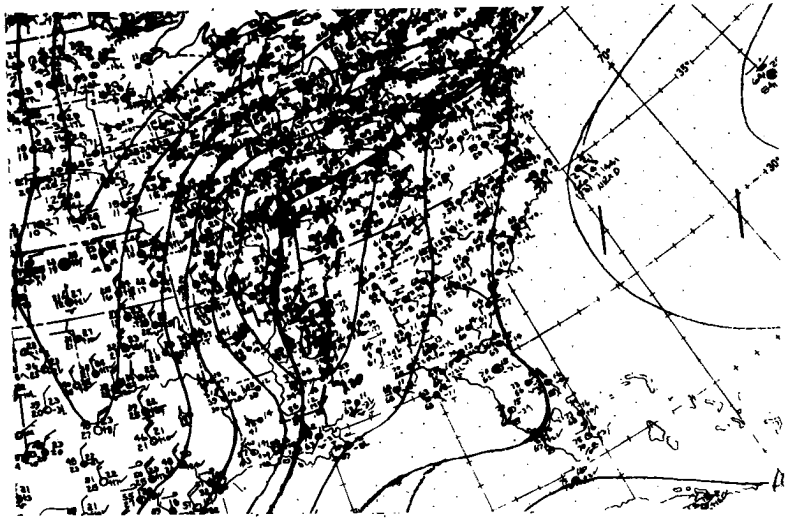

SURFACE

Figure 2c. Surface, 850 mb, and 500 mb for 27 Jan 1967 00Z showing development of the storm system.

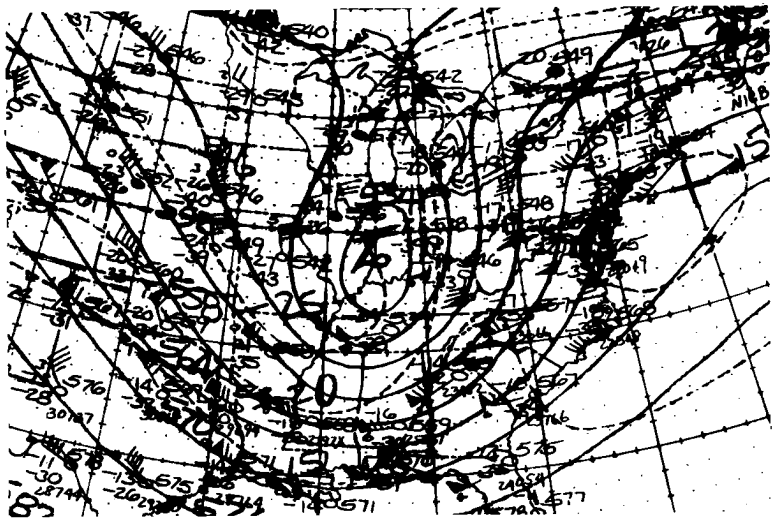

500mb

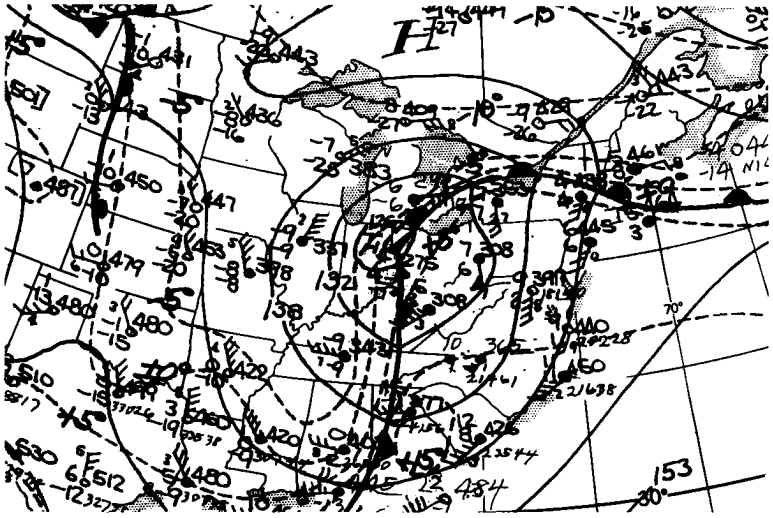

850mb

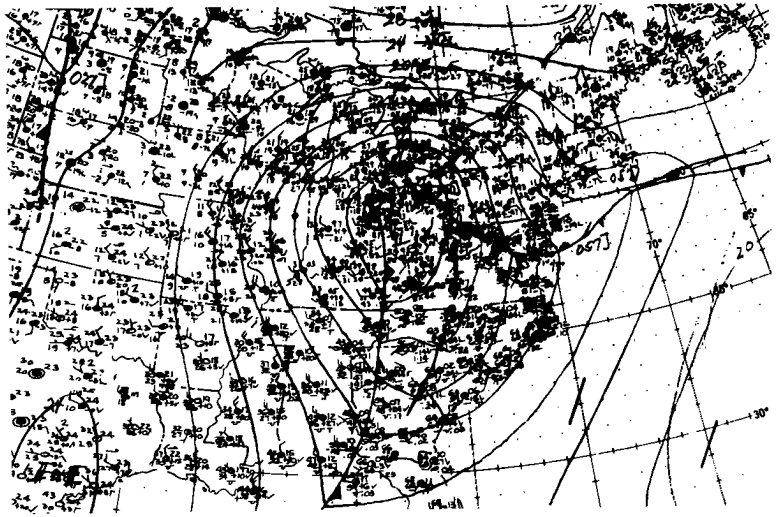

SURFACE

Figure 2d. Surface, 850 mb, and 500 mb for 27 Jan 1967 12Z showing development of the storm system.

CHAPTER III

PRECIPITATION ANALYSIS

The total storm precipitation from this storm generally ranged from about 1/2" to 2 3/4" for individual stations. The greatest amounts were recorded in the narrow belt running from central Missouri, across lower Lake Michigan and southern Michigan state. The total snowfall within this belt ranged from ten inches to 24 inches (figure 3).

Plots of cumulative precipitation verses time have been drawn for various stations (fig. 4 a-b). These charts clearly show that there is a similarity in the time distribution of precipitation among stations within the snowbelt, and a marked difference from those outside the snowbelt. At Chicago and Flint, both in the snowbelt, there was continuous precipitation for 29 hours and 28 hours, respectively. South of the snowbelt - ie. Dayton and Indianapolis - in spite of being closer to the storm center, total precipitation was much less with most of the accumulation a result of periodic heavy showers. These stations also show the highly variable nature of the pre-warm front precipitation. The total time over which the precipitation was occuring at Dayton and Indianapolis was about the same as for stations within the snowbelt. The abrupt decrease in precipitation north of the snowbelt is shown by Rockford, Illinois, and Houghton Lake, Michigan. At a distance of less than 100 miles from the center of the snowbelt, accumulations were relatively insignificant.

The spatial distribution of precipitation ahead of the warm front was such that the heaviest precipitation occured at the extreme edge of the precipitating area. This is contrary to the more normal pattern calling for the heaviest precipitation to occur nearest the surface

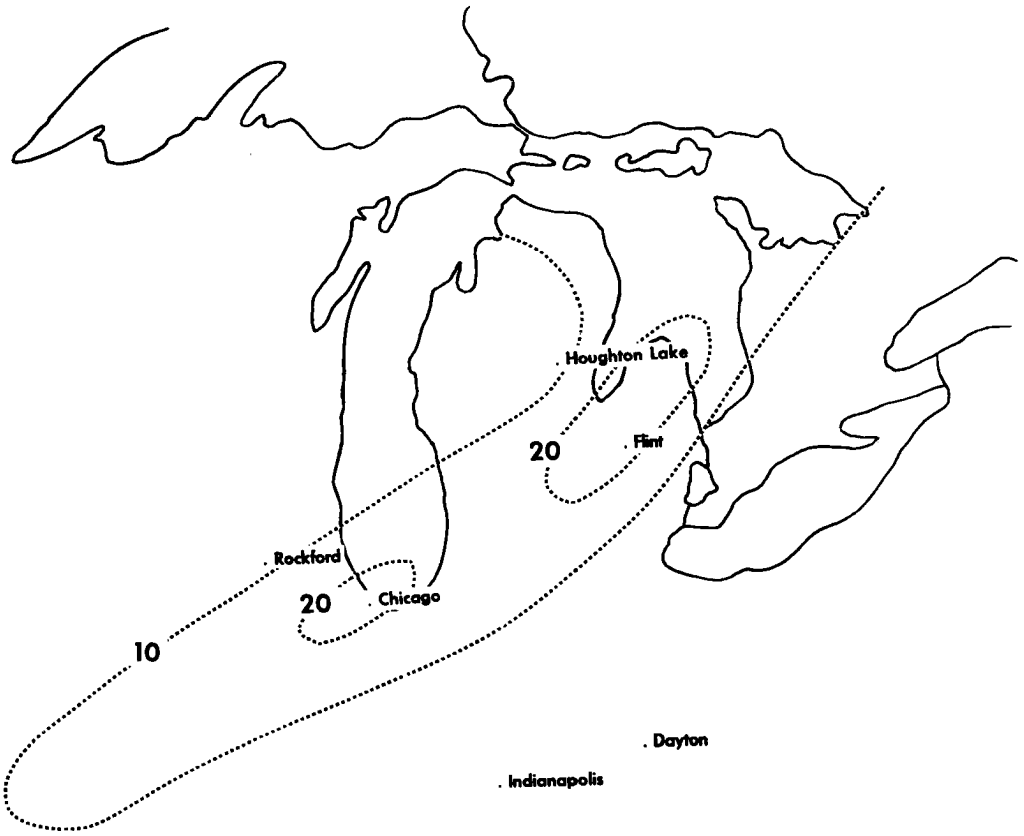

Figure 3. Location of the heavy snow belt. The hourly rain gauge stations shown are used for the comparisons in figure 4. Units are in inches of snowfall.

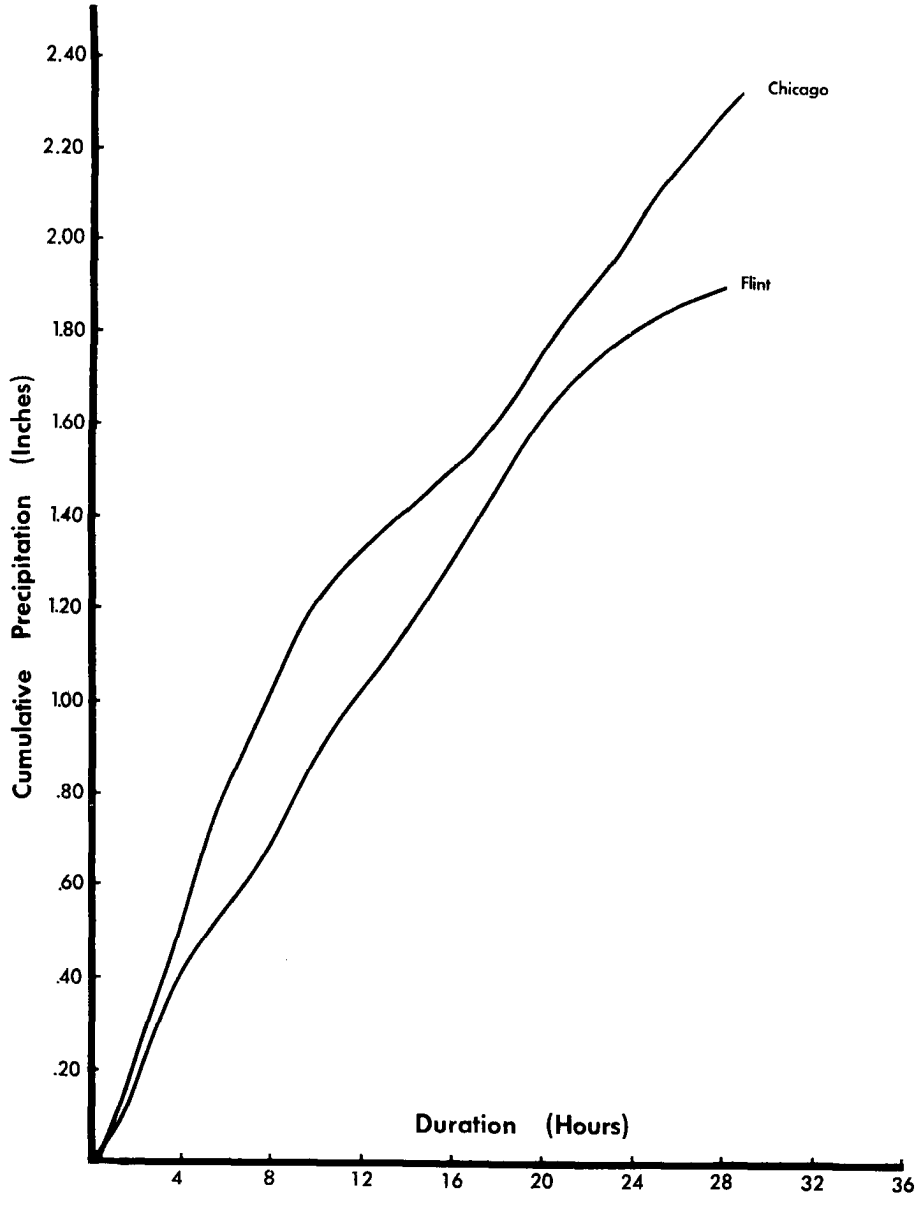

Figure 4a. Plot of cumulative precipitation vs. duration of precipitation. For station locations see figure 3.

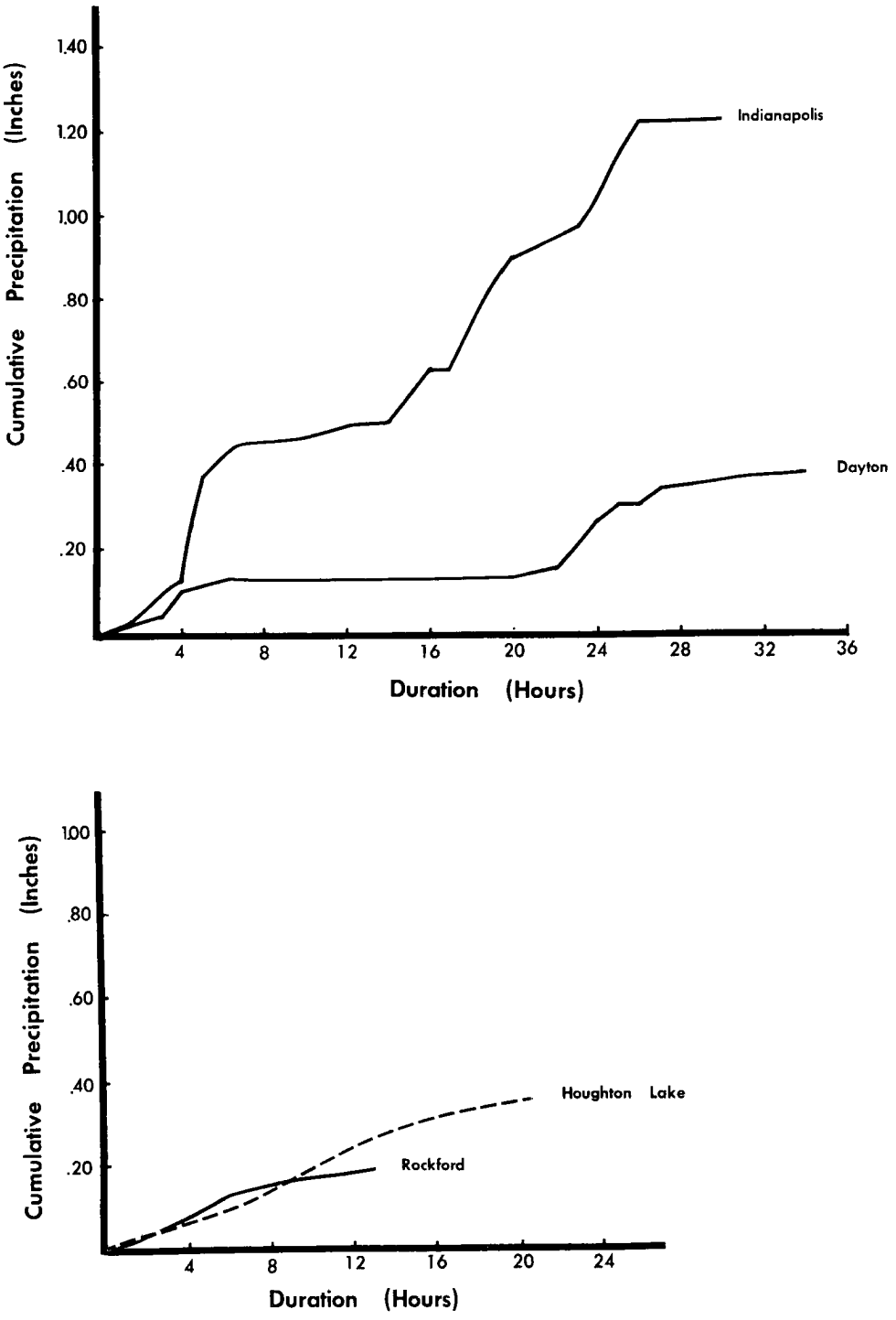

Figure 4b. Same as figure 4a.

front, with then a general decrease in intensity farther ahead. In the absence of any topographical influences, the mechanism causing this precipitation anomaly must be vertical instability.

CHAPTER IV

ISENTROPIC ANALYSIS

It is often convient to represent the motion of the atmosphere on substantial surfaces. Such surfaces have a distinct advantage over more conventional surfaces, such as isobaric, in that the three-dimensional flow pattern is directly observable. If the atmospheric motion is dry adiabatic, surfaces of constant potential temperature (θ) are considered as a substantial surfaces, while if condensation-precipitation processes are occuring, surfaces of constant equivalent potential temperature (θ_e) or constant wet-bulb potential temperature (θ_w) can be used.

The methods used in this investigation are basically the same as that employed by Green, Ludham, and McIlveen (1966), who used θ-surfaces, or that of Harrold and Nicholls (1968), and Browning and Harrold (1969), who used θ_w-surfaces.

In this study, actual winds were plotted on surfaces of constant equivalent-potential temperature. θ_e-surfaces were used because our main interest is in the regions of ascending air where condensation and precipitation are likely to occur and θ_e is more nearly conserved during such a process.

θ_e analyses were carried out at 12 hour intervals between 26/12Z and 27/12Z inclusively, and at 5°K intervals between θ_e = 275°K and θ_e = 320°K. The θ_e = 325°K surface corresponds closely to the tropopause and no computations were made above this level.

Streamline analyses on the θ_e surfaces, shown in figure 5, reveal the nature of the instantaneous motions in the various sections of the storm. The θ_e = 290°K surface for 26/12Z is representative of motions in the cool air mass just under the advancing warm front. On this

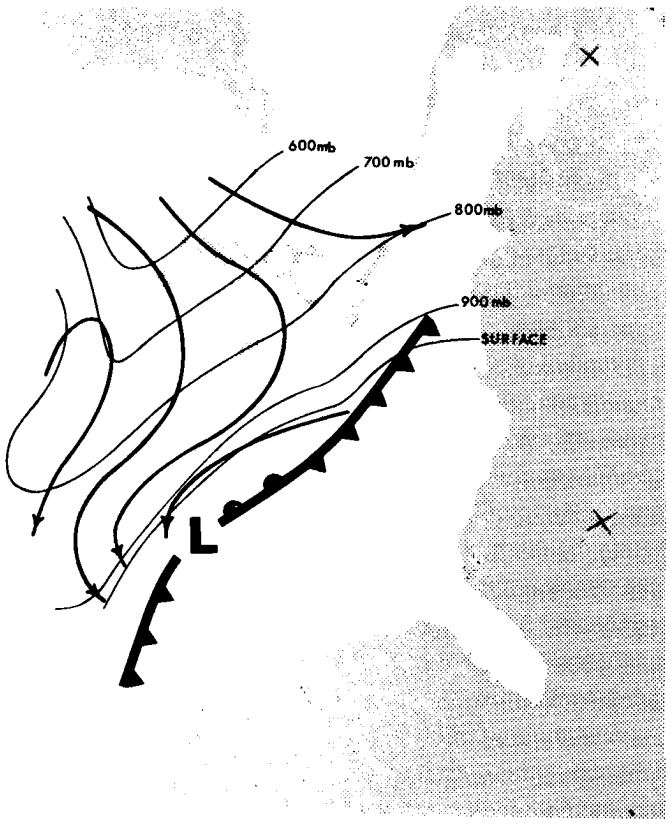

Figure 5a. Pressure contours (thin lines) on the Θ_e = 290°K surface for 26/12Z. Thick solid lines are streamlines.

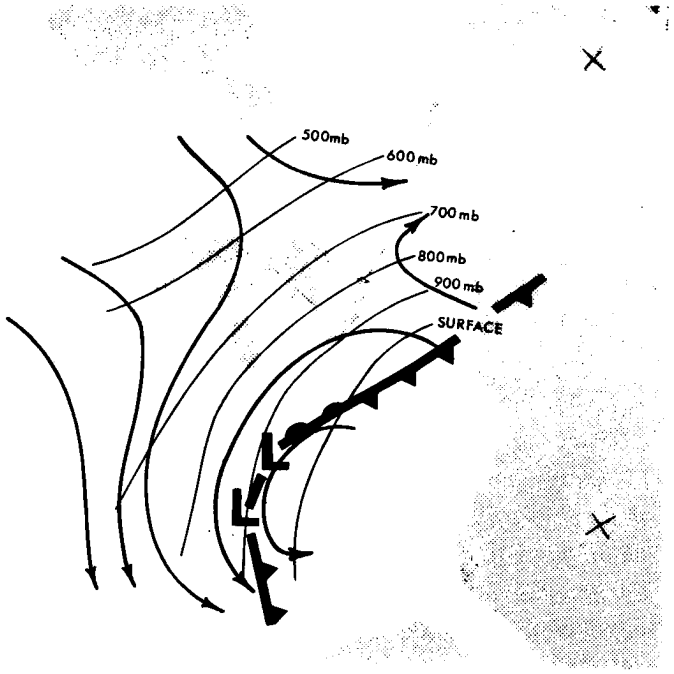

Figure 5b. Same as for figure 5a. except for Θ_e = 295°K, 27/00Z.

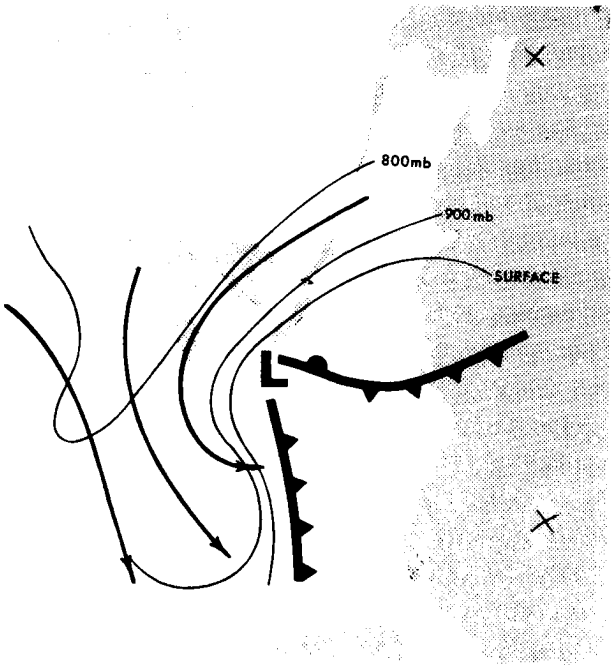

Figure 5c. Same as for figure 5a. except for Θ_e = 285°K, 27/12Z.

surface there is general decent at all levels up to 600 mb. The Θ_e = 295°K for 27/00Z is typical of the pattern of motions found just above the warm front, with widespread ascent to about 700 mb, and descending air above this level. The Θ_e = 285°K surface for 27/12Z is representative of motions in the fresh outbreak of polar air behind the cold front. The motions on this surface show descending air at all pressure levels to above 600 mb, with marked lateral spreading of the streamlines below 800 mb.

These broad scale patterns of motions are consistent with those prescribed by the Norweigian model, and consistant with the results of other investigations (Palmén and Newton, 1951: Reiter, et al, 1965: Harrold and Nicholls, 1968: and Browning and Harrold, 1969).

As can be seen from figure 6, there is a close correspondence between the regions of ascent and areas of cloudiness. The area of cloudiness is assumed to be the region where relative humidities exceed 95%.

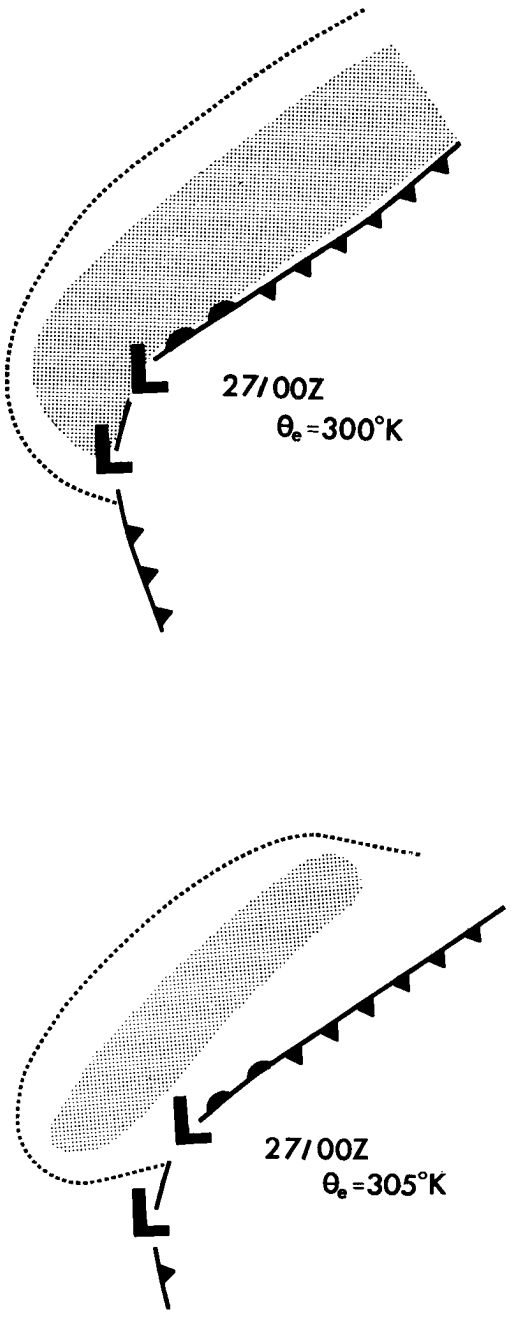

Figure 6. Location of region of broad scale ascent with respect to storm center for selected times. Gray shaded area is the region of cloudiness (RH $\geq$ 95%). Dashed line marks the extent of ascending air.

CHAPTER V

VERTICAL MOTION

Since the low level wind maximum has been shown to be related to the region of heavy precipitation, vertical motions were calculated for the region surrounding this wind maximum. In these calculations a natural coordinate system has been employed as a frame of reference in which the s-axis is tangent to the flow on the isentropic surface, along which s increases in the direction of flow, and the n-axis is perpendicular to the flow, along which n increases to the left of the direction of flow. Pressure, p, is taken as the vertical axis, decreasing upwards.

If $p = p(t, s, \Theta_e)$, then

$$\frac{dp}{dt} = \left(\frac{\partial p}{\partial t}\right)\left(\frac{dt}{dt}\right) + \left(\frac{\partial p}{\partial s}\right)\frac{ds}{dt} + \left(\frac{\partial p}{\partial \Theta_e}\right)\left(\frac{d\Theta_e}{dt}\right) \qquad [5\text{-}1]$$

The last term in equation [5-1] is the diabiatic heating term and consists of the radiational cooling of the atmosphere. Since this cooling amounts to less than $3^{\circ}C$ per day the diabatic heating term can be considered as negligible. Thus, equation [5-1] can be reduced to

$$\omega = \frac{dp}{dt} = \frac{\partial p}{\partial t}\Big)_{\Theta_e} + \frac{\partial p}{\partial s}\Big)_{\Theta_e} V_s \qquad [5\text{-}2]$$

This equation shows that the vertical motion of an individual parcel of air is comprised of the local vertical movement of the isentropic surface, and the vertical component of the quasi-horizontal wind due to the slope of the isentropic surface in the direction of a streamline.

A time increment of only 3 hours was used in calculating vertical motions for two reasons. First, for short periods of time streamlines can be used instead of trajectories, and second, the errors resulting from Θ_e not being totally conserved during a process are small.

An 8° latitude square grid consisting of 15 points was centered on the position of the low level wind maximum such that the center column of points was normal to the flow (figure 7).

For the 26/12Z time period, $\left(\frac{\partial p}{\partial t}\right)_{\theta_e}$ was calculated and found to contribute insignificantly to the overall pattern of vertical motion, and so was neglected in computations for the remaining two time periods.

The vertical motion was then found by assuming that a parcel of air originating at each of the grid points with a given speed would be moved along a trajectory for a distance corresponding to the distance traversed in a three hour period at that particular speed. The magnitude of the vertical motion in a three hour period was then the difference between the final and the initial pressure of the trajectory.

The results of these calculations are shown in figure 8. Above the warm front (θ_e = 290°K) there was persistant upward motion in the left rear quadrant of the wind maximum. The magnitude of this ascent, corresponding to the broadscale ascent of warm moist air up the warm front, was around 40mb/3hrs with extreme values exceeding 100mb/3hrs. By 27/12Z, the low level wind maximum, and hence the grid, had lagged behind the storm center so that it shows little of the ascending warm air.

To the right of the low level wind maximum and in the cold air mass, there was decending air, with a magnitude of about 20mb/3hrs. Palmén and Newton (1951) found similar values (maximum of 125mb/12hrs.) in an outbreak of polar air over the continental United States.

For the 26/12Z and 27/00Z time periods there is a close agreement between the region of calculated upward vertical motion and areas where precipitation was occurring at the ground (figure 8). There are fringe

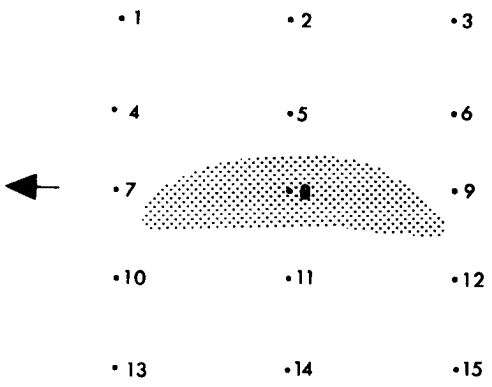

Figure 7. Fifteen point grid system used in the analysis. Gray shaded area is the location of the core of maximum wind. Downstream direction is to the left.

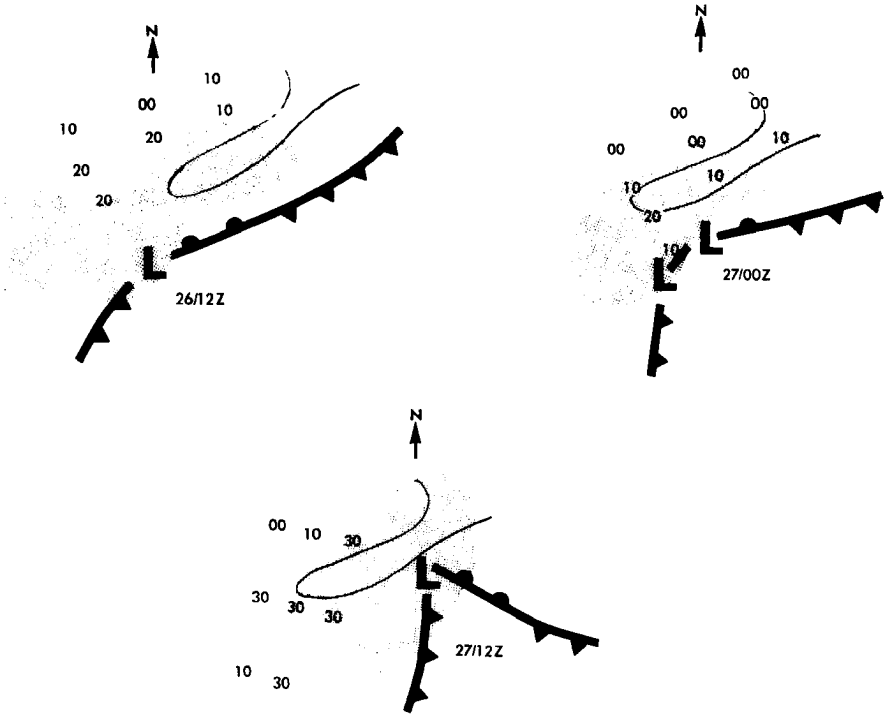

Figure 8a. Magnitude of vertical motion in mb/3hrs. for each of the time periods for the θ_e = 280°K surface. The gray shaded area is the region where precipitation was occurring at that map time. Thick solid line outlines the belt of heavy snowfall. The thin line separates the ascending ($\omega<0$) region from the decending ($\omega>0$) region.

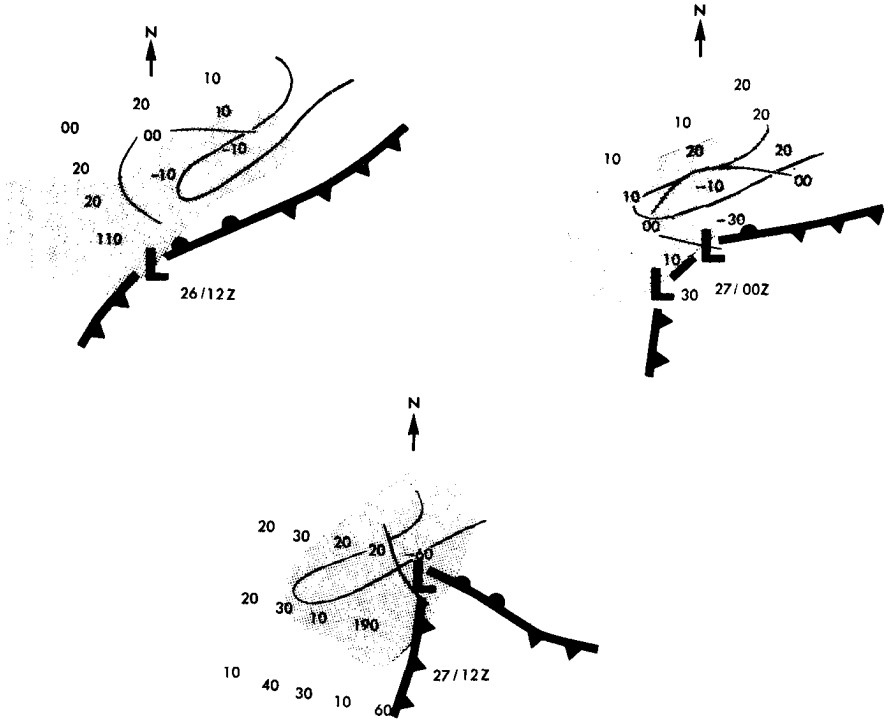

Figure 8b. Same as for figure 8a. except Θ_e = 290°K.

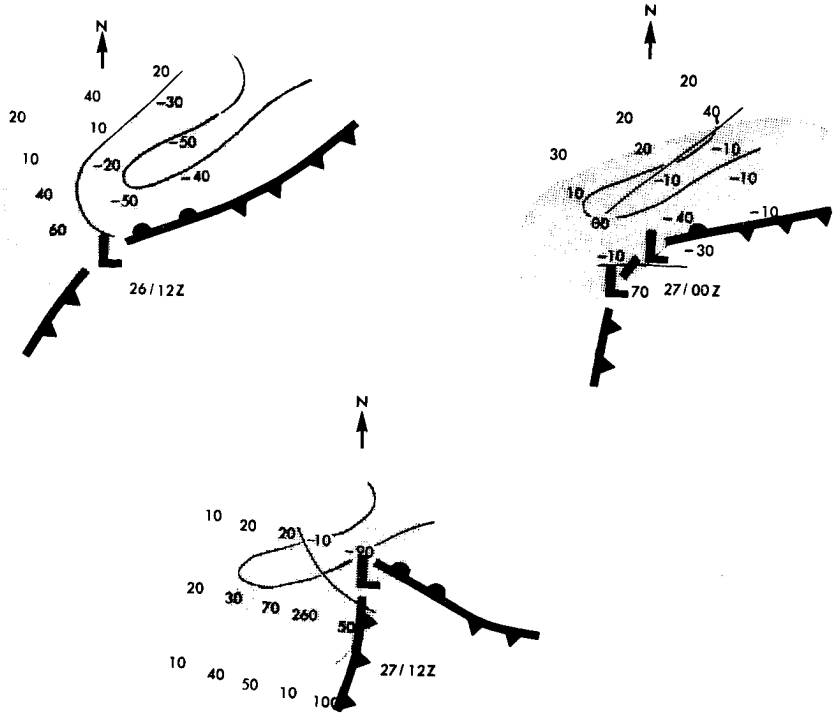

Figure 8c. Same as for 8a. except Θ_e = 300°K.

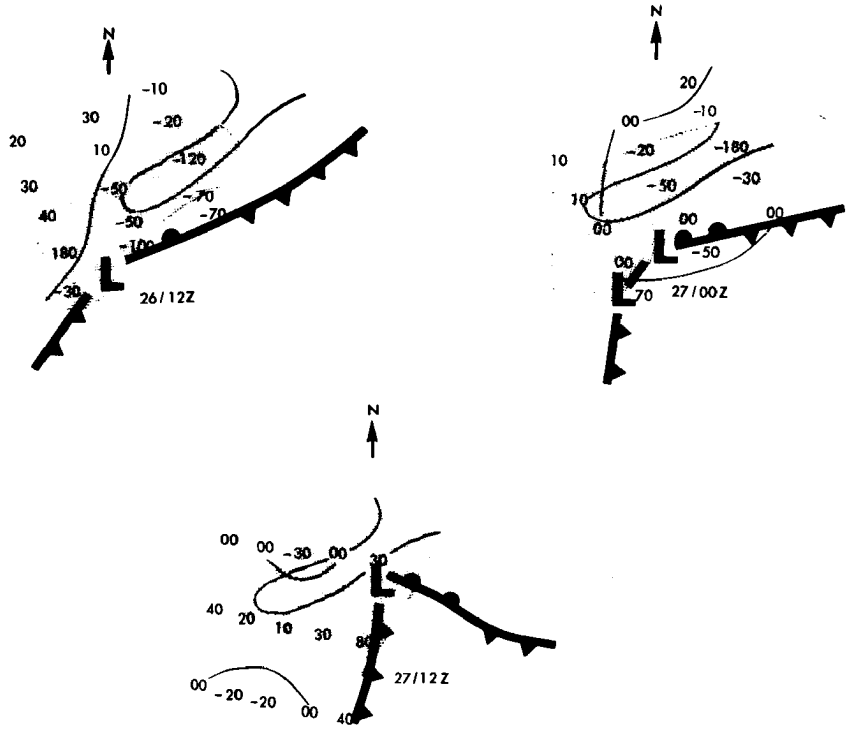

Figure 8d. Same as for figure 8a. except for Θ_e = 310°K.

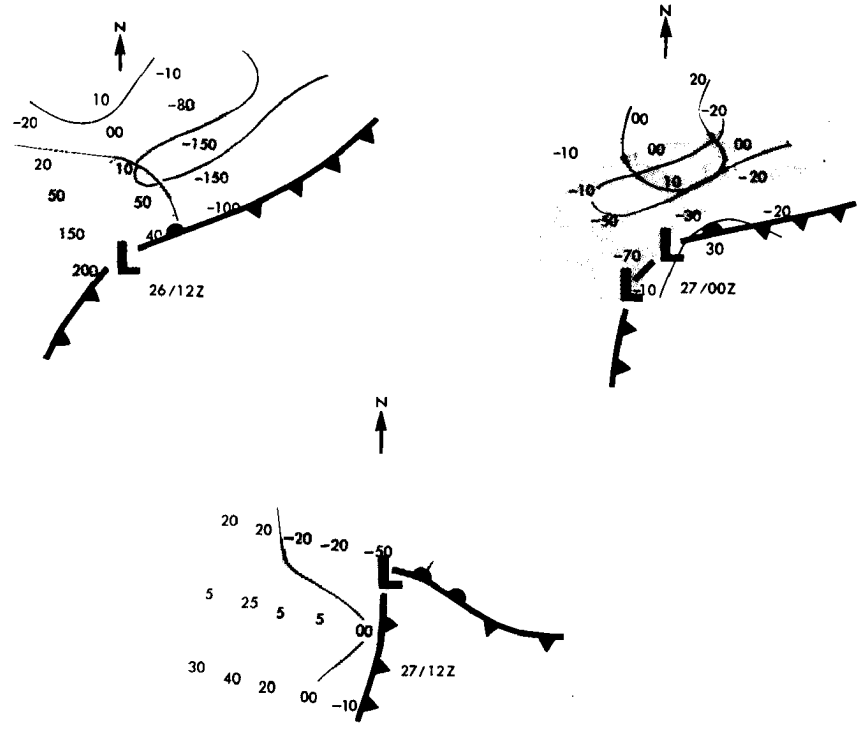

Figure 8e. Same as for figure 8a. except Θ_e = 320°K.

areas of light precipitation in regions where there is descent, but the areas of heaviest precipitation definitely occur where there is ascent over a deep layer.

The discrepancy between the area of precipitation and vertical motion can possibly be explained by the occurance of shower activity in an otherwise decending region (Rasmussen, et. al, 1969).

The magnitude of error in calculating vertical velocities by the above method, as well as by all other methods, was estimated to be ± 50% (Browning and Harrold, 1969). This error is a result of the uncertainty in the orientation of the Θ_e surfaces caused by inaccuracies in measuring relative humidities as well as by the existence of the large depths of constant Θ_e and the severe folding and distortions of the Θ_e surfaces that are possible.

CHAPTER VI

PRODUCTION OF VERTICAL INSTABILITY

As was pointed out earlier, in the absence of any topographical influences, the mesoscale precipitation patterns are a result of localized areas of vertical instability. Such is the case for this late January storm.

A mechanism whereby the needed vertical instability is produced will now be developed, and then applied directly to the case under investigation.

Potential vorticity is a conservative property for an individual parcel of air during adiabatic motion, assuming frictionless flow and no differential heating (Reiter, 1963). The development of the form of potential vorticity used here follows that of Haltiner and Martin (1957). The equations for frictionless motion in isentropic coordinates (x,y,θ,t) are given by

$$\frac{\partial u}{\partial t} + u\frac{\partial u}{\partial x} + v\frac{\partial u}{\partial y} + \frac{\partial u}{\partial \theta}\frac{d\theta}{dt} = -\frac{\partial \psi}{\partial x} + fv \qquad [6\text{-}1a]$$

$$\frac{\partial v}{\partial t} + u\frac{\partial v}{\partial x} + v\frac{\partial v}{\partial y} + \frac{\partial v}{\partial \theta}\frac{d\theta}{dt} = -\frac{\partial \psi}{\partial y} - fu \qquad [6\text{-}1b]$$

Where $\psi = C_p T + gz$.

Assuming $\frac{d\theta}{dt} = 0$, differentiating (1a) and (1b) with respect to y and x, respectively, and subtracting (1a) from (1b) yields the isentropic vorticity equation.

$$\frac{d\zeta_\theta}{dt} = -\zeta_\theta \nabla_\theta \cdot v \qquad [6\text{-}2]$$

where ζ_θ is the absolute vorticity. The equation of continuity in isentropic coordinates is given by

$$\nabla_\theta \cdot v = \left(\frac{\partial p}{\partial \theta}\right)^{-1} \frac{d}{dt}\left(\frac{\partial p}{\partial \theta}\right) - \frac{1}{\delta\theta}\left(\frac{d\delta\theta}{dt}\right) \qquad [6\text{-}3]$$

The last term on the right is the diabatic heating term and is relatively small and can be neglected. Substituting [6-3] into [6-2] gives

$$\zeta_\theta^{-1} \frac{d\zeta_\theta}{dt} = \left(\frac{\partial p}{\partial \theta}\right)^{-1} \frac{d}{dt}\left(\frac{\partial p}{\partial \theta}\right)$$

or

$$\ln\zeta_\theta - \ln\left(\frac{\partial p}{\partial \theta}\right) = \text{constant}$$

Therefore [6-4]

$$\ln\left[\zeta_\theta \left(\frac{\partial p}{\partial \theta}\right)^{-1}\right] = \text{constant}$$

In order for equation [6-4] to be true the quantity in brackets must be constant. Therefore

$$\frac{d}{dt}\left[\zeta_\theta \left(\frac{\partial p}{\partial \theta}\right)^{-1}\right] = 0$$

or

$$\frac{d}{dt}\left[\zeta_\theta \left(\frac{\partial \theta}{\partial p}\right)\right] = 0 \qquad [6\text{-}5]$$

Physically, equation [6-5] means whenever the vorticity of a parcel of air is increasing with time, there must be a corresponding decrease in the lapse rate of θ and hence the stability, of that parcel of air.

The conservation of potential vorticity as derived above is applicable to dry adiabatic motion. However, the same concepts can be used during moist-adiabatic motion. The only difference between the θ-system (dry) and the θ_e-system (moist) is that the latter incorporates the diabatic heating due to the release of latent heat into the system, while the former does not. This shift to the θ_e coordinates is then justifiable as long as bouyant ascent does not occur. This restriction is necessary because if bouyant ascent takes place there would be large volumes of atmosphere with constant θ_e and $\frac{\partial \theta_e}{\partial p}$ would approach zero and equation [6-5] would become meaningless.

The above concept of conservation of potential vorticity can now be applied to this particular storm with good results. A region of

strong positive vorticity is produced by the low level wind maximum discussed earlier. Located at about the 850 mb on the warm-front in a cycloncially curving flow the left rear quadrant of the wind maximum is the region of maximum vorticity increase and strong convergence.

As can be seen from figure 9 a parcel of air originating near the surface front in the warm air is lifted up the warm-front into a region of increasing cyclonic vorticity. As the vorticity of the parcel of air increases, there must be a corresponding decrease in its stability. Since the stability of the parcel is initially close to neutral (figure 10), the combined effect of decreasing stability and convergence results in a region of subsynoptic scale instability and overturning of the air in the left rear quadrant of the box.

Unfortunately the methods used to calculate vertical motions are capable of showing only the broad scale features of the flow pattern, and cannot show the scale of vertical motions generated by the mesoscale instability. However as a result of this instability, there must be an isolated region of heavier precipitation as measured at the ground. The density of surface hourly rain gauge data is sufficient to allow an isohyetal analysis on a subsynoptic scale in order to locate this region of suspected instability. The results of this analysis are shown in figure 11. For the 26/12Z time period the region of heaviest precipitation is found in the left front quadrant of the box. Referring back to figure 9 for 26/12Z it can be seen that there is strong convergence associated with the low pressure center situated in the right front quadrant of the box. The convergence results in the strong vertical motion near the low center and the heavy precipitation.

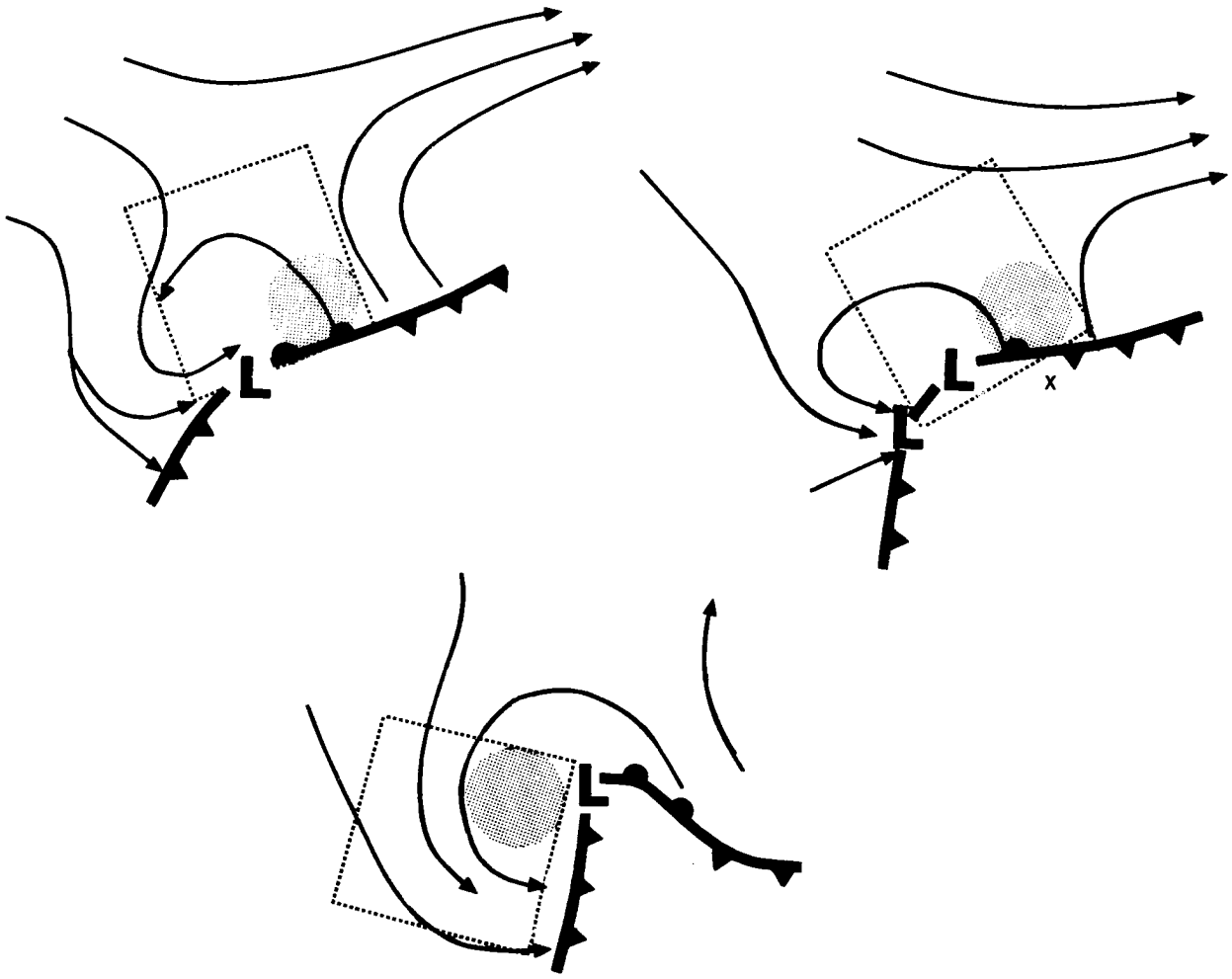

Figure 9. Location of the region of increasing cyclonic vorticity along a streamline (shaded area) for the θ_e = 305°K surface for each time period.

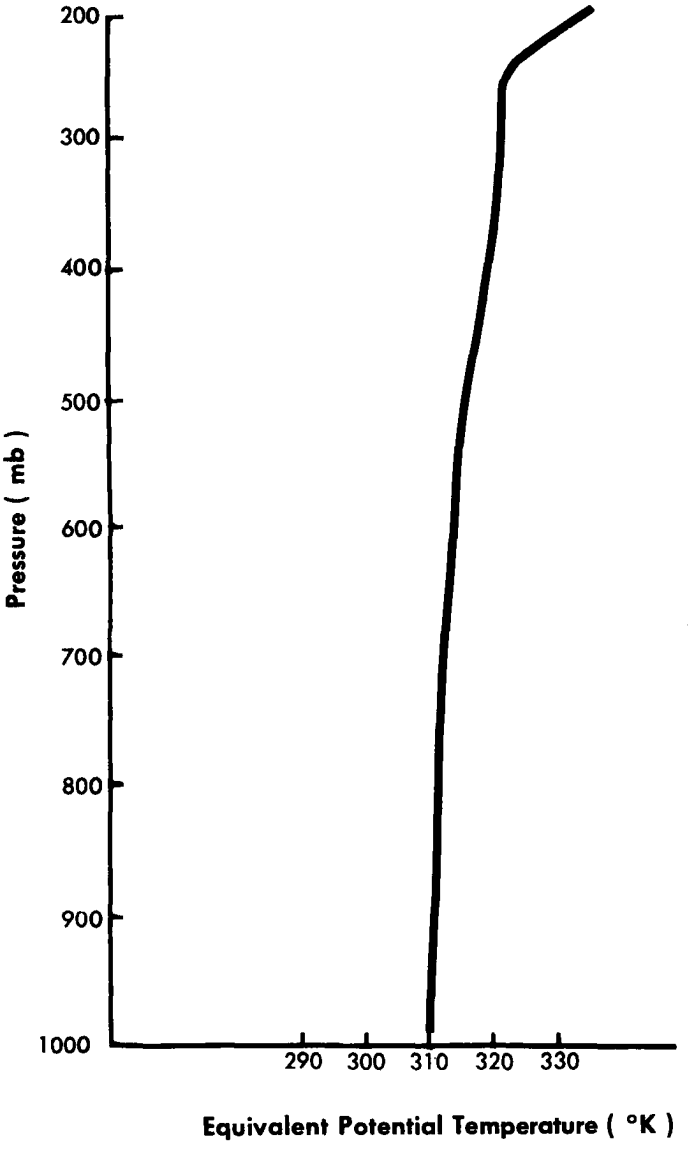

Figure 10. Representative vertical profile of Θ_e for the warm air sector of the storm. Location of sounding is shown by a 'x' in figure 9.

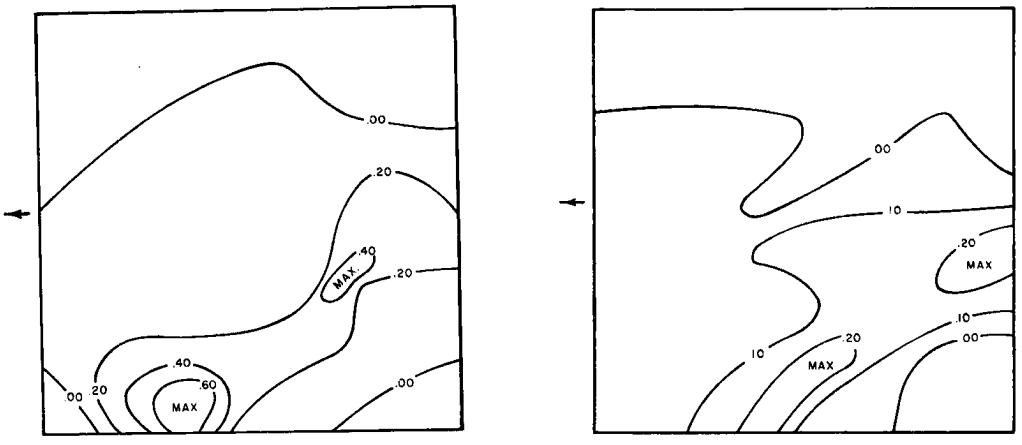

26/12Z

27/00Z

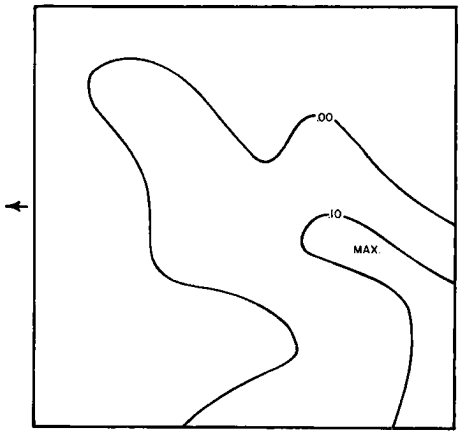

27/12Z

Figure 11. Area averaged precipitation pattern within the 8° latitude box. Units are inches/3hrs.

If we neglect this particular precipitation maximum as being caused by dynamically induced convergence and vertical motion, the region of heaviest precipitation at this time period and subsequent time periods is found in the left rear quadrant of the box. This is exactly where the heaviest precipitation is expected to be found based on the production of vertical instability as discussed above.

The marked decrease in the amount of precipitation occurring within the box between the last two time periods is caused by the relative movement of the region of ascending warm moist air away from the low level wind maximum.

It can be concluded that our model calling for the production of instability and an isolated region of heavier precipitation in the left rear quadrant of the low level maximum is valid for this single case.

CHAPTER VII

CALCULATION OF MOISTURE TRANSPORT

The moisture transport through the box was calculated to answer two questions. First, is it possible to determine the precipitation over the box from the flux of water vapor through the box, and if so, which θ_e levels contribute the most toward the precipitation?

The atmospheric water balance equation may be written as (Palmén, 1967)

$$P-E = -\frac{1}{\rho_w A}\frac{\partial}{\partial t}\int_{p_o}^{p_t} qdA\,\frac{dp}{g} - \frac{1}{\rho_w A}\int_{p_o}^{p_t}\oint_l V_n q dl\,\frac{dp}{g}. \qquad [7\text{-}1]$$

Where

P = precipitation

E = evaporation from the earth's surface

q = specific humidity

ρ_w = density of water

p_o = pressure at the earth's surface

p_t = pressure at the top of the atmosphere

A = area

V_n = component of wind normal to the boundary.

It is assumed that the time rate of change and divergence of flux of liquid water and ice through the atmospheric volume is negligible compared to the vapor terms (Palmén, 1967; Rasmussen, 1968).

Both terms on the right hand side of equation [7-1] are easily calculated from aerological data and their residual is the quantity P-E. In the final calculations, the evapotranspiration from the earth's surface during the winter season during periods of heavy precipitation is assumed to be very much smaller than the precipitation that was occurring, and so was neglected.

The results of this calculation are summarized in Table 1. The gauge precipitation (P_G) is an area averaged value of the amount of precipitation that fell during that three hour period of evenly distributed over the entire area of the box. For the first two time periods precipitation occured in about 2/3 of the total area of the box, while at the last time period, precipitation occured over less than 1/2 of the total area.

TABLE 1

Results of Precipitation Calculation
cm/3hrs

	P_F	P_w	P	P_G	P/P_G
26/12Z	0.21	0.00	0.21	0.28	.75
27/00Z	0.09	0.01	0.10	0.15	.67
27/12Z	0.02	0.02	0.04	0.05	.80

The calculated values of precipitation are considered as reasonable and within the limits for this kind of calculation for two reasons. First, the precipitation was found as the residual of two larger terms, and second, it was an attempt to measure a mesoscale phenomenon with synoptic scale data.

Vertical profiles of the divergence of moisture flux term for the three time periods were drawn (figure 12). For 26/12Z and 27/00Z, almost exclusively the total contribution toward precipitation was from the Θ_e = 305°, 310° and 320°K surfaces. These three surfaces are above the warm front boundary and air that is being brought into the box on these surfaces originates in the warm sector of the storm and has a high moisture content.

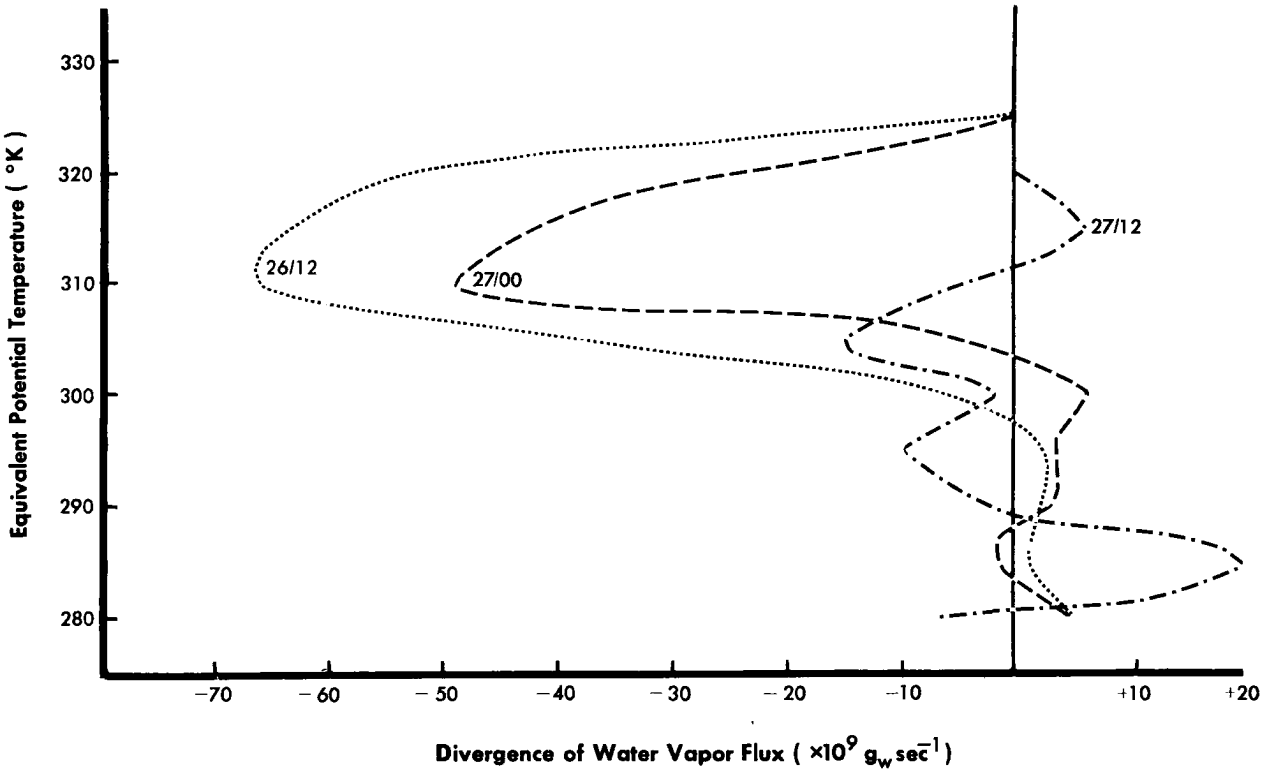

Figure 12. Vertical profiles of the divergence of water vapor flux for each θ_e channel for each time period.

CHAPTER VIII

CONCLUSION

The development of this particular late January storm follows in classical Norweigian Cyclone model. Assuming Θ_e conserved there was found to be decending air at all levels in the cold air mass and an active region of uplift over the warm front.

Embedded within the precipitation area ahead of the warm-front is a small region of heavier precipitation. The mesoscale precipitation distribution is caused by an isolated region of convective instability. The instability acted to only increase the intensity of the already occuring precipitation, and not to increase the duration of the precipitation.

The mechanism for generating this instability was found to be a low level wind maximum producing a region of maximum vorticity increase in the left rear quadrant of the wind maximum. As the warm, moist air is lifted up the warm-front by the broad scale flow pattern, the absolute vorticity of a parcel of air is increased, resulting in decreased stability. Further lifting produces instability and a mesoscale region of heavier precipitation. The necessary condition persist for more than 24 hours so that the net result is the long and narrow belt of unprecendented snowfall. By 27/12Z the storm center has moved away from the low level wind maximum so that its affect on the ascending air is small and the heavy precipitation ended.

The precipitation was calculated as a residual from the atmospheric water balance with good results. The ratio of calculated precipitation to measured precipitation averaged .74 for the three time periods. This leads to confidence in the analysis of the aerological data,

which is critical in the methods used for calculating vertical motions.

In light of the success with which the concept of conservation of potential vorticity was applied to a particular storm to determine its precipitation pattern, it is felt that further studies of additional cases of abnormally heavy precipitation are justifiable and necessary. Such a study would help to establish the relative importance of such a mechanism in the precipitation processes of wintertime midlatitude cyclones.

Bibliography

Arakawa, H., 1956: Characteristics of the low-level jet stream. Journal of Meteorology, 13(5), 504-506.

Barad, M. J., 1961: Low altitude jet stream. Scientific American, 205(2), 120-131.

Bonner, W. D., 1965: Statistical and kinematic properties of the low level jet. University of Chicago, Dept. of Geophysical Science SMRP No. 38, 54 pp.

_____, 1966: Case study of thunderstorm activity in relation to the low level jet. Monthly Weather Review, 94(3), 167-178.

_____, 1968: Climatology of the low level jet. Monthly Weather Review, 96(12), 833-850.

_____, S. Esbensen, and R. Greenberg, 1968: Kinematics of the level jet. Journal of Applied Meteorology, 7(3), 339-347.

Boucher, R. J., 1959: Synoptic-physical implications of 1.25cm vertical-beam radar echoes. Journal of Meteorology, 16, 312-326.

Browning, K. A., and T. W. Harrold, 1969: Air motions and precipitation growth in a wave depression. Quarterly Journal of the Royal Meteorological Society, 95, 288-309.

Bunting, J. and D. Lamb, 1968: Heavy snow in the Chicago area as revealed by satellite pictures. University of Chicago SMRP No. 75, 49 pp.

Danielson, E. F., 1961: Trajertories: isobaric, isentropic, and actual. Journal of Meteorology, 18, 479-486.

_____, and R. Bleck, 1966: Research in four-dimensional diagnosis of cyclonic storms. Contract No. AF 19(628)-4762, The Pennsylvania State University, 52 pp.

Findlater, J., 1966: Cross-equatorial jet streams at low levels over Kenya. Meteorological Magazine, 95(1133), 353-364.

Gerhardt, J. R., 1962: An example of a nocturnal low level jet stream. Journal of the Atmospheric Sciences, 19(1), 116-118.

_____, 1963: Mesoscale association of a low level jet stream with a squall line-cold front situation. Journal of Applied Meteorology, 2(1), 49-55.

Green, J. S. A., F. H. Ludlam, and J. F. R. McIlveen, 1966: Isentropic relative-flow analysis and parcel flow. Quarterly Journal of the Royal Meteorological Society, 92, 210-219.

Haltiner, G. J. and F. L. Martin, 1957: Dynamical and Physical Meteorology, New York, McGraw-Hill, 454 pp.

Harrold, T. W., and M. J. Nicholls, 1968: An investigation of air motion in frontal precipitation. Meteorological Office Scientific Paper Nos. 29, 46 pp.

Hoecker, W. H., 1963: Three southerly low level jet systems delineated by the Weather Bureau special pibal network of 1961. Monthly Weather Review, 91(10/12), 573-582.

_____, 1965: Comparitive physical behavior of southerly boundary layer wind jets. Monthly Weather Review, 93(3), 133-144.

Izumi, Y., 1964: Evolution of temperature and velocity profiles during breakdown of a nocturnal inversion and a low level jet. Journal of Applied Meteorology, 3(1), 70-82.

_____, and H. A. Brown, 1966: Temperature, humidity, and wind variations during dissipation of a low level jet. Journal of Applied Meteorology, 5(1), 36-42.

Jones, D. E., 1966: A note on the use of hourly rainfall observations. Meteorological Magazine, 95, 325-332.

Joseph, P. V., and P. L. Raman, 1966: Existence of low level westerly jet stream over peninsular India during July. Indian Journal of Meteorology, 17(3), 407-410.

Means, L. L., 1954: A study of the mean southerly wind maximum in low levels associated with a period of summer precipitation in the Middle West. Bulletin of the American Meteorological Society, 35(4), 166-170.

Palmén, E., and C. W. Newton, 1951: On the three-dimensional motions in the outbreak of polar air. Journal of Meteorology, 8, 25-39.

_____, 1967: Evaluation of atmospheric moisture transport for hydrological purposes. Report No. 1, WMO, International Hydrological Decade Projects, Geneva, 63 pp.

Petterssen, S., 1956: Weather Analysis and Forecasting Volume 1. New York, McGraw-Hill, 428 pp.

Pitchford, K. L., and J. London, 1962: The low level jet as related to nocturnal thunderstorms over Midwest United States. Journal of Applied Meteorology, 1(1), 43-47.

Rasmussen, J. L., 1968: Atmospheric water balance of the Upper Colorado River Basin. Atmos. Science Paper No. 121, Dept. of Atmos. Science, Colorado State University, Fort Collins, 121 pp.

Rasmussen, J. L., et. al., 1969: Moisture analysis of an extratropical cyclone. Archive for Meteorology, Geophysics, and Bioclimatology Series A., 18, 3-4 275-289 pp.

Reiter, E. R., 1963: Jet-stream Meteorology, Chicago, University of Chicago Press, 515 pp.

_____., et. al. 1965: Effect of large mountain ranges on atmospheric flow patterns as seen from Tiros satellites. Colorado State University, Atmospheric Science Technical Paper No. 69, 110 pp.

Rossby, C.-G. and collaborators, 1937: Isentropic analysis. Bulletin of the American Meteorological Society. 18, 201-209.

Saucier, W. J., 1955: Principles of Meteorological Analysis, Chicago, The University of Chicago Press, 438 pp.

Sawyer, J. S., 1952: A study of the rainfall of two synoptic situations. Quarterly Journal of Royal Meteorological Soceity, 78, 231-246.

Smith, J. S., 1967: The great Chicago snowstorm of 1967: Weatherwise, 20, 249-253.

Staley, D. O., 1960: Evaluation of potential-vorticity changes near the tropopause and the related vertical motions, vertical advection of vorticity, and transfer of radioactive debris from stratosphere to troposphere. Journal of Meteorology, 17(6), 591-620.

Wallington, C. E., 1963: Mesoscale patterns of frontal rainfall and clouds. Weather, 18, 171-181.

Wexler, H., 1961: Boundary layer interpretation of the low level jet. Tellus, 13(3), 368-378.

Wexler, R., and D. Atlas, 1959: Precipitation generating cells. Journal of Meteorology, 16, 327-332.